PROCEEDINGS OF SPIE

SPIEDigitalLibrary.org/conference-proceedings-of-spie

Mesoporous silica nanoparticles for treating spinal cord injury

Désirée White-Schenk, Riyi Shi, James F. Leary

Désirée White-Schenk, Riyi Shi, James F. Leary, "Mesoporous silica nanoparticles for treating spinal cord injury," Proc. SPIE 8587, Imaging, Manipulation, and Analysis of Biomolecules, Cells, and Tissues XI, 858716 (22 February 2013); doi: 10.1117/12.2004916

SPIE.

Event: SPIE BiOS, 2013, San Francisco, California, United States

Mesoporous silica nanoparticles for treating spinal cord injury

Désirée White-Schenk[a, b,e], Riyi Shi[c,d,e], James F. Leary[b,d,e]
[a]Interdisciplinary Biomedical Sciences Graduate Program; [b]Birck Nanotechnology Center; [c]Center for Paralysis Research; [d]Department of Basic Medical Sciences, School of Veterinary Medicine; [e]Weldon School of Biomedical Engineering
Purdue University, West Lafayette, Indiana

ABSTRACT

An estimated 12,000 new cases of spinal cord injury (SCI) occur every year in the United States. A small oxidative molecule responsible for secondary injury, acrolein, is an important target in SCI. Acrolein attacks essential proteins and lipids, creating a feed-forward loop of oxidative stress in both the primary injury area and the surrounding areas. A small molecule used and FDA-approved for hypertension, hydralazine, has been found to "scavenge" acrolein after injury, but its delivery and short half-life, as well as its hypertension effects, hinder its application for SCI. Nanomedical systems broaden the range of therapeutic availability and efficacy over conventional medicine. They allow for targeted delivery of therapeutic molecules to tissues of interest, reducing side effects of untargeted therapies in unwanted areas. Nanoparticles made from silica form porous networks that can carry therapeutic molecules throughout the body. To attenuate the acrolein cascade and improve therapeutic availability, we have used a one-step, modified Stober method to synthesize two types of silica nanoparticles. Both particles are “stealth-coated” with poly(ethylene) glycol (PEG) (to minimize interactions with the immune system and to increase circulation time), which is also a therapeutic agent for SCI by facilitating membrane repair. One nanoparticle type contains an amine-terminal PEG (SiNP-mPEG-Am) and the other possesses a terminal hydrazide group (SiNP-mPEG-Hz). The former allows for exploration of hydralazine delivery, loading, and controlled release. The latter group has the ability to react with acrolein, allowing the nanoparticle to scavenge directly. The nanoparticles have been characterized and are being explored using neuronal PC-12 cells *in vitro*, demonstrating the potential of novel silica nanoparticles for use in attenuating secondary injury after SCI.

Keywords: Mesoporous silica nanoparticles, acrolein, hydralazine, nanomedicine

1. INTRODUCTION

1.1 Spinal cord injury (SCI)

SCI and traumatic brain injury (TBI) are traumas to the central nervous system (CNS). Motor vehicle accidents most heavily contribute to the occurrence of CNS injuries. Since young adults and teens are most likely to be involved in these types of accidents, their age group is significantly affected.[1] Aside from possible mortality, injury usually results in impaired motor capabilities (e.g. paralysis), sensory capabilities (e.g. hypersensitivity and hyposensitivity), and/or neurologically-based pain. This can drastically reduce a patient’s quality of life and place a large burden on society, both in health care costs and lost productivity.

Acrolein, a reactive oxygen species (ROS), has been implicated in secondary injury in neuronal tissues.[2,3] Other studies have explored the various biochemical changes caused by acrolein in neuronal tissues, including lipid peroxidation, myelin damage, and mitochondrial damage.[4-6] Acrolein's primary carbon can undergo nucleophilic attack, but contributing to its destructive nature, the electrophilic (electron deficient) carbons of the π-bond (second bond of C=C) can undergo attack by nucleophiles in the cell. Specifically, acrolein reacts with sulfur-containing lysine residues, histidines, and unsaturated fatty acids.

When acrolein attacks fatty acids, more acrolein is generated in a cycle of uncontrolled lipid peroxidation.[7] When acrolein reacts with lipids, such as those in the cell membrane, the membrane is compromised, and more acrolein is released to attack other tissue in a feed forward process. This creates a cascade of oxidative stress to a particular area of injury. In this way, acrolein can increase the stress and damage healthy tissues surrounding the injury site.[4,8,9] The large amount of oxidative stress overwhelms the body's natural anti-oxidant, glutathione.[10] Normally, glutathione is oxidized,

Imaging, Manipulation, and Analysis of Biomolecules, Cells, and Tissues XI, edited by Daniel L. Farkas, Dan V. Nicolau, Robert C. Leif, Proc. of SPIE Vol. 8587, 858716

which stops ROS and reactive nitrogen species (RNS) from oxidizing proteins and structures in the cell. It then would be reduced to its original form by glutathione reductase. In a large area of oxidation, glutathione cannot be reduced quickly enough to account for the overwhelming, cyclic, and unchecked production of acrolein.

Fortunately, the drug hydralazine, which is commonly used to treat hypertension, has been found to "scavenge" for acrolein and other oxidative species.[4,8,11–14] Particularly, the drug will scavenge and react with acrolein that has reacted with proteins.[4] As mentioned earlier, the carbonyl group in acrolein is free for nucleophilic attack. Once acrolein reacts with a protein, the carbonyl is free, and hydralazine can attack it. The reaction results in a Schiff-base, imine (C=N bond) formation, which the body uses regularly for amino acid synthesis. When the drug reacts with free acrolein, it reduces the amount of acrolein that can induce lipid peroxidation, arresting the feed forward production of acrolein. Ultimately, stopping the process would allow cells to recover more effectively and minimize long-term damage.

Long-chain polymers have also been studied in SCI. Poly(ethylene) glycol (PEG) and chitosan have both been studied for their effects on treating the effects of SCI and other neurological diseases.[9,13–15] The polymers first plug the damaged membrane by associating with the holes. The interaction of the polymers then causes the two separated parts of the membrane to associate with each other, effectively closing the hole and stopping the invasion of unwanted ions and molecules.[9,15]

1.2 Nanomedicine

In biology and medicine, nanotechnology has developed rapidly in the last decade to create a new segment of nanotechnology: nanomedicine. Major goals of the field involve the improvement of drug delivery, diagnostic or imaging techniques, and theranosis, which is a combination of both. Additionally, as the field broadens, it expands to include nanopharmacology and nanotoxicity for the exploration of how the body reacts to the new, nano-sized structures.

The composition of nanoparticles is extremely diverse. They have been synthesized using a wide range of materials: metal (e.g. gold, silver, cadmium), metal oxides (iron oxide, titanium oxide, zinc oxide), silica, polymers, biological molecules (peptides and DNA), among others.[16–19] As the field has progressed, more nanoparticles are being made from mixtures of these materials, which provide new benefits and functions for the various applications that a single material will not possess. The multi-functional nanoparticles become a unique nanomedical system used to address a biological problem.[20]

1.3 Using silica-PEG nanoparticles for targeting SCI

Therefore, this study explored silica-based nanoparticles with PEG for ultimately scavenging acrolein to attenuate secondary injury after SCI. Ultimately, PEG will associate with the membrane in injured tissue, serving to target to injured neurons, and repair the membrane damaged caused by acrolein. Once there, the hydralazine can be delivered in the area, scavenging acrolein and attenuating the oxidative stress. The nanoparticles are made using a facile, one-step synthesis that incorporates PEG directly onto the nanoparticles. For the purpose of functionality, two different PEG products were used, and both types of nanoparticles were characterized.

2. MATERIALS AND METHODS

2.1 Synthesis of PEG-amine modified silica nanoparticles

The silica nanoparticles were synthesized using a modified Stöber method.[21,22] 20 mg of amine- modified methoxy poly(ethylene) glycol (mPEG-Am) MW5000 (0.004 mmol) (Sigma, St. Louis) was dissolved in 6 mL of methanol. Upon dissolution, 64 uL of tetramethylorthosilicate (0.434 mmol) (TMOS, Sigma, St. Louis) was added. Drop wise, 750 uL of 2 M NaOH (1.5 mmol) was added to the mixture while agitating. The solution was vortexed at 25°C for 1 hour. To remove most of the solvent, the milky solution was added to a 30 kDa Amicon membrane filter (Millipore, Billerica, MA) and centrifuged for 15 minutes at 2800 g. The filtrate was removed, and 5 mL of nanograde water was added to the filter and spun again for 10 minutes. The solution was aged for 15 days before 3 mL of nanograde water was added to the filter and spun for 15 minutes. Residual methanol was removed via evaporation. Concentration of the nanoparticle solution was obtained gravimetrically by solvent evaporation under vacuum. For use in cell culture, the nanoparticle samples were sterile filtered using a 0.2 μm syringe filter and diluted to appropriate concentrations in phosphate buffered saline (PBS).

2.2 Synthesis of PEG-hydrazide modified silica nanoparticles

Synthesis proceeded as described for mPEG-Am modified particles. mPEG-hydrazide MW5000 (mPEG-Hz) was obtained from Laysan Bio, LLC (Arab, AL).

2.3 Size measurements and stability

The dynamic light scattering (DLS) of nanoparticles was measured in both nano-grade water and PBS using a Zetasizer NS (Malvern, United Kingdom) at 25°C and 37°C. Each measurement was taken four times to create an average result. The monodispersity index of the nanoparticles was also determined to avoid conditions where the nanoparticles would aggregate. For stability measurements, the samples were stored at 25°C and measured at various time points. Upon loss of volume, 200 uL of the appropriate solvent (water or PBS) was added to the sample before measuring.

2.4 Zeta potential

The interaction of all particles in aqueous media is governed by the "zeta potential" of both the cells and the nanoparticles. The nanoparticles were measured in both nano-grade water and PBS at pH 7 using a Zetasizer NS (Malvern, UK) at 25°C and 37°C. Each measurement was taken three times to create an average result. Since zeta potential includes the particle-associated counter-ions attracted to the particle or cell from the medium, the zeta potential will be different in water versus PBS. Ultimately it should be measured in a medium similar to that of the cells and/or particles in-vivo to best predict the actual nanoparticle-cell interactions.

2.5 Fourier Transform Infrared (FTIR) spectroscopy

As synthesized nanoparticle samples were previously suspended in nano-grade water. Amine-terminated methoxy PEG was dissolved in nano-grade water. Ten uL of nanoparticle or PEG solution was placed onto a crystal KBr card (International Crystal Laboratories, NJ) and allowed to dry. Before running samples, a water background was obtained. Each spectra was obtained with 256 scans on a Nicolet FTIR (Thermo Scientific) and processed using KnowItAll Informatics System (Bio-Rad). The FTIR spectra were used to examine specific bond arrangements important to the correct overall assembly of the nanoparticles and conjugated molecules.

2.6 Reflective hyperspectral imaging

Samples for reflective hyperspectral imaging (RHI) were sent to Cytoviva, Inc in Arab, AL. For PEG modification on the nanoparticles, nanoparticles with and without PEG were sent for spectral analysis, along with PEG alone. The spectra were compared and both silica nanoparticles and PEG were mapped in the PEGylated nanoparticle sample. Similar analysis was also performed on nanoparticles loaded with 75 mM of hydralazine. This form of particle-based RHI is a rapid means of determining if different molecules are co-associated spatially and can be done on nanoparticles below the imaging optical limit in aqueous media without resorting to electron microscopy (EM) which must be done under vacuum conditions that can introduce artifacts. This form of RHI, unlike EM, can also see structures that are not electron dense.

2.7 Hydralazine loading

For hydralazine loading, 3 mg of the synthesized mPEG-Am in PBS was shaken with 75 mM solution of hydralazine hydrochloride (Sigma, St. Louis) in PBS.

2.8 Cell culture of PC-12 cells

Rat PC-12 cells were obtained from American Tissue Culture Collection (ATCC, Manassas, Virginia) and cultured in suspension in T-25 or T-75 flasks with RPMI-1640 (ATCC) media containing 10% heat-inactivated equine serum and 5% fetal bovine serum (FBS). The cells were co-cultured twice per week and seeded in concentrations from 1:4 to 1:2.

2.9 Lactate dehydrogenase (LDH) cell permeability assay

LDH activity gives a measure of cell's membrane integrity. As the membrane is damaged, cytosolic LDH is released from the cell. The LDH Toxicology Kit was purchased from Sigma and used per the manufacturer's instructions. PC-12 cells were seeded in triplicates at 5 x 10^5 cells/mL in reduced-serum media (RPMI-1640 with 5% heat-inactivated horse serum) to reduce background created by serum activity. The cells were incubated with the various compounds for 24 hours before analyzing the growth medium for LDH activity. After incubation, the LDH activity was measured using a

VersaMax microplate reader (Molecular Devices, LLC, Sunnyvale, CA). The data is reported as a change of LDH activity compared to the vehicle control, calculated as follows:

$$Percent\ change\ (\%) = \frac{(Test_{490\text{-}690} - Control_{Average(490\text{-}690)})}{Control_{Average(490\text{-}690)}} * 100$$

2.10 Statistical analysis

To determine statistical significance, ANOVA was performed on each data set. For pair-wise comparisons, a test using the Least Significant Difference (LSD) was used. P-values less than 0.01 were considered significant.

3. RESULTS AND DISCUSSION

3.1 Characterization of mPEG-Am modified nanoparticles

The silica nanoparticles were prepared to incorporate the polymer into the silica network (Figure 1), which eliminates an additional PEGylation step that is common in many other synthesis schemes.[12,23–26] The "stealth" polymer, generally designed to prevent the deposit of proteins on its surface to minimize interactions with the immune system and increase circulation time, made be conjugated to a functional group present in the original nanoparticles or grafted via electrostatic interactions. In the former schemes, an additional organosiloxane, generally containing an amine or carboxylic acid derivative, is added with the precursor (TMOS or TEOS) to functionalize the particles. The PEG, functionalized with a reactive moiety, is then conjugated to the particles.[25] The PEG content relies on the functionalization with the organosiloxane, and depending on whether the organosiloxane modification occurs during or after initial particle formation, the synthesis requires two to three steps. With PEG grafting, the PEG coats the nanoparticles via electrostatic interactions.[24,26] Over time, the PEG may dissociate from the silica particles, or the coatings may become uneven. In the current study, the PEG serves a dual purpose. PEG is nanomedicine's "stealth" molecule, as it has been shown to prevent opsonization.[17,27] Specifically for spinal cord injury, PEG serves as a target for injured neurons and associates with them, aiding in membrane repair.[9]

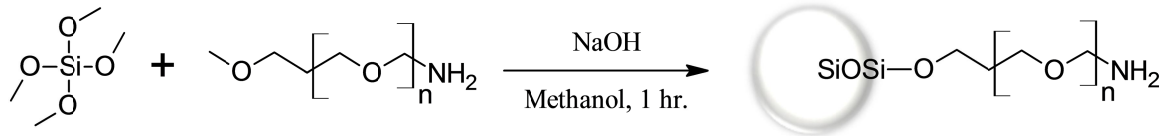

Figure 1. Synthesis scheme of Si-mPEG NP's. The silica precursor, TMOS, is hydrolyzed and condensed with methoxy-PEG and TMOS. Condensation with TMOS allows the nanoparticle network to grow whereas condensation with mPEG stops the growth of the particle.

In the one-step synthesis, the PEGylation is a function of its hydrolysis and condensation with the siloxane. Furthermore, the Stöber method creates water and alcohol as by-products, eliminating the need to remove the organic solvents and surfactants in emulsion techniques. Volatile alcohols are fast and easy to remove. Inorganic surfactants used to synthesize silica particles require harsh, acidic environments to remove them from the surface of the silica particles.[28–30] Ma et al. recently reported a synthesis technique using a combination of the Stöber and emulsification methods.[31] The synthesis and purification was performed at 30°C and utilized a surfactant with an alcohol and water solvent system. Especially for use in biological systems and scaling procedures, eliminating side products and steps may make production much faster, easier, and cheaper.

To confirm the synthesis technique, the particles were analyzed using Fourier transform infrared spectroscopy (FTIR). The technique relies on the vibration of chemical bonds in a sample using IR. It can be used to compare samples based on the formation or disappearance of particular bonds and/or functional groups in the different samples. In this study, unmodified nanoparticles and mPEG alone were analyzed and compared to mPEG-containing particles (Figure 2). In the plain particles (Figure 2A), silica esters bonds are shown the 1300-1000 cm^{-1} region and the same peak appears in the PEGylated sample (Figure 2C), but it has broadened and contains shoulders from the fingerprint region (900-800 cm^{-1}) of the PEG. Lastly, a weak, broad band has appeared around 2900 cm^{-1} of the PEGylated sample, which is indicative of C-H stretching.

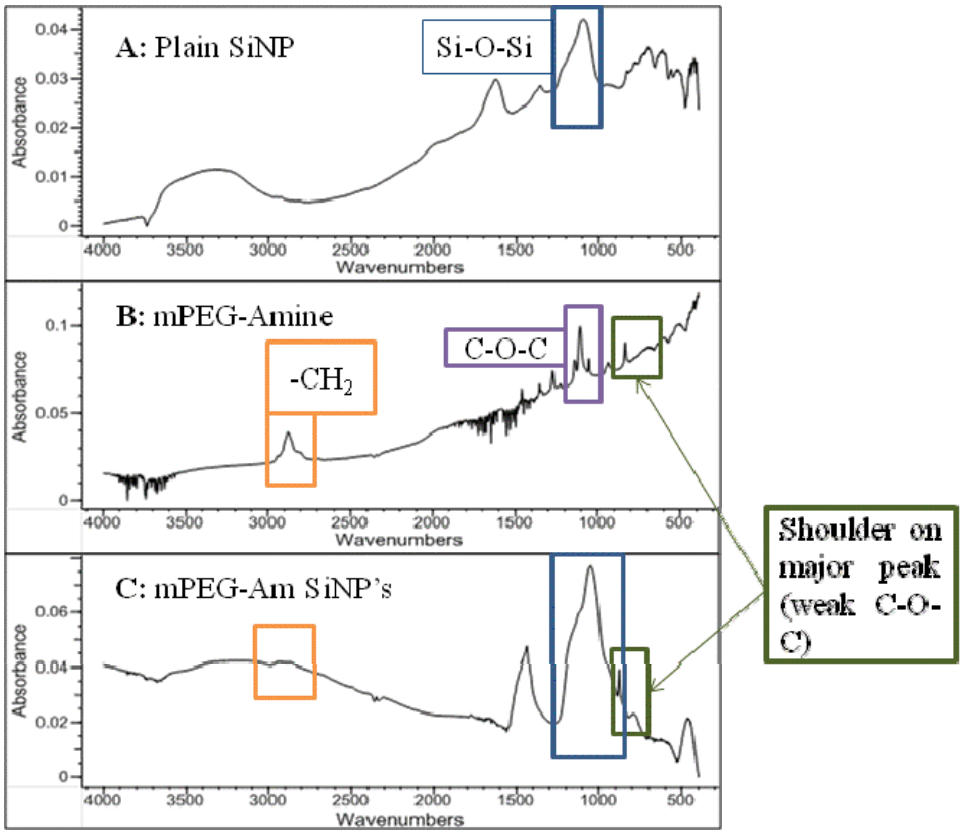

Figure 2. FTIR spectra of A) Non-PEGylated nanoparticles, B) mPEG-Amine, and C) mPEG-Amine modified nanoparticles. The bare nanoparticles show characteristic peaks of silica-ester bonds in 1200 cm^{-1} region (A), which overwhelms the smaller peaks of the mPEG-Am alone (B) on the PEG-modified particles (C). The PEGylated particles show a slight broadening in the ester region (1300-1000 cm^{-1}), which is indicative of Si-O-C bonds after condensation during synthesis.

To corroborate the FTIR data, samples were sent to Cytoviva, Inc. for reflective hyperspectral imaging. To obtain a spectrum, the technique relies on collecting the reflected light from a sample to show spatial co-assocciation of different molecules. For the analysis, PEG and nanoparticles with and without PEG were analyzed. From there, the PEGylated sample was analyzed and using the control spectrum, "mapped" for the presence of PEG and silica particles (Figure 3). The PEGylated sample shows the presence of PEG and silica juxtaposed. The spectrum of each sample is also different. In the PEGylated sample, the spectrum has shifted towards the peak of the PEG sample, indicating a change in the reflectance pattern of the sample that could be attributed to the presence of PEG.

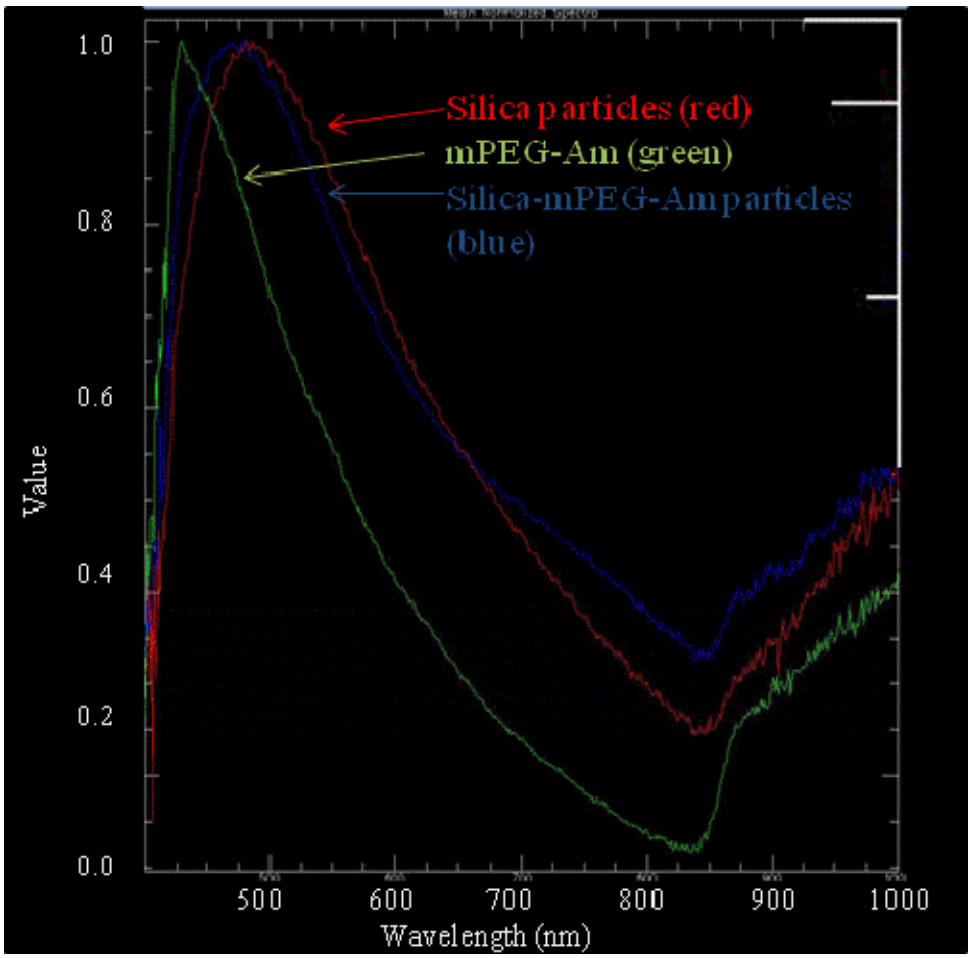

Figure 3. Spectral maps of mPEG alone (left), non-PEGylated sample (right) and Si-mPEG sample (middle). The PEGylated sample shows a shift towards the mPEG spectra that may be attributed to PEG.. Images provided by Cytoviva, Inc. (Arab, AL).

The synthesized particles were collected and measured using dynamic light scattering (DLS). Specifically for nano-type applications, size, stability, and zeta potential are all important characteristics. Therefore, determining these characteristics are important if the particles are to be used clinically. For instance, the body has natural size and charge (zeta potential) filters, including the kidneys, liver, and spleen. Each of these organs will remove particles of various sizes and charges, and in order for the particles to be effective, they should be tailored to fall within a range that avoids excessive uptake by these organs.[32]

Dynamic light scattering (DLS) measures the radius a particle appears to have in solution. Components of a solvent or buffer form a layer that moves with the nanoparticle, forming the "hydrodynamic radius". As a particle moves through solution (Brownian motion), it scatters light that can be collected. A large particle moves slower and scatters less light while a smaller particle moves more quickly in comparison. Obviously, since the particles are moving in a fluid, the solvent properties, specifically viscosity, changes their motion in the fluid system. Based on DLS measurements, the particles have an average hydrodynamic diameter of 21.33 nm and a polydispersity index (PDI) of 0.085, indicating a monodisperse population (Figure 4). The PDI gives an indication of a sample's population distribution, ranging from 0.00-1.00. A high PDI usually indicates various size populations in one sample. The samples were stored at room temperature in the sample cuvette and measured over time. Even after long periods of time, the particles retain their integrity. They can also be diluted into PBS and retain their integrity, but they begin to aggregate after only six months.

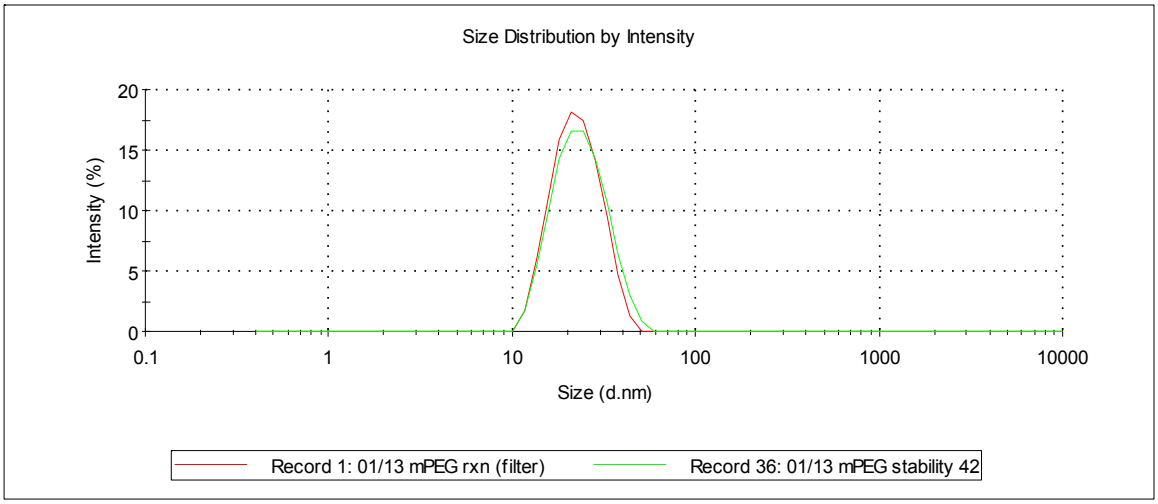

Figure 4. Size of Si-mPEG-Am NP's in aqueous solution after synthesis and after 42 weeks (10 months) of shelf storage. The sample was pulled directly after synthesis and filtered through a 0.2 um. Subsequent measurements were taken of the same sample over time.

Directly after removing the organic solvent, the pH of the nanoparticle solutions is about 10 from the base catalyst. The particles are stable in the solution, but for biological purposes, the pH must be adjusted. To account for this change, the particle solutions were diluted, pH-adjusted, and their properties were measured at a neutral pH in both water and PBS.

Zeta potential deals with how the particles arrange charges in a solution, which can affect how the particles will interact with cells. It may affect the pathway the particles undergo. On the other hand, they could either stick heavily to the cell membrane or be repelled by the charge arrangements. Zeta potential also gives an indication of how the particles interact with each other. A neutral, or zero, zeta potential indicates instability and association of the nanoparticles with each other, which usually leads to aggregation –something highly undesirable, especially in clinical applications.

Table 1. Size and Zeta potential of mPEG-Am modified nanoparticles

Temp. (ºC)	Solution	Diameter (nm)	PDI	Zeta Potential (mV) (St. Dev.)	Zeta of Non-PEG sample (mV)
25	Water	24.78	0.147	-29.2 (1.7)	-31.7 (6.9)
25	PBS	24.19	0.121	-25.0 (2.3)	-25.4 (1.2)
37	Water	24.07	0.131	-26.2 (1.1)	-29.3 (0.7)
37	PBS	23.28	0.129	-21.9 (0.8)	-23.4 (0.8)

The PDI increases once the pH has been adjusted, which is likely due to a change in both the ionic strength and pH. In more acidic conditions, the positively charged hydrogen ions are attracted to the negatively charged surface of the nanoparticle becoming part of the associated counter-ion cloud and slightly lowering the zeta negativity of the zeta potential. The zeta potential is negative, likely due to the various silanol groups on the surface of the nanoparticle. To prevent non-specific sticking of the nanoparticles to the cells, which are almost always negatively charged with a zeta potential of approximately 10-20 mV, we want the nanoparticles to themselves be at least slightly negatively charged zeta potential of about -5 to -10 mV. Targeting molecules, in this case the attraction of PEG for cell membrane lipids, will overcome a slight electrostatic barrier between the nanoparticles and the cells to produce a good targeting effect to injured cells. The PEG creates a shielding effect, which changes with the temperature and ionic strength. For instance, polymer interactions often change with temperature, and those changes are mostly absent in the non-PEGylated sample. The effect of the solution is seen less at room temperature, but at body temperature, the zeta potential increases in both water and PBS, which may be accounted for in the ion concentration difference between water and PBS. PBS contains more ions to create a plane around the particles, offsetting the high negative charge. The PEGylated sample also has a low ratio of amine groups that can contribute to changing the charge around the particle, which is not present in the non-PEGylated sample.

3.2 Hydralazine loading of the mPEG-Am modified nanoparticles

Hydralazine has been shown to scavenge for acrolein; therefore, loading the nanoparticles provides a therapy that will stop the secondary injury cascade, which affects both the injured and surrounding healthy tissue, caused by acrolein. Reflective hyperspectral imaging was used to confirm loading of hydralazine. A sample of the nanoparticles loaded with hydralazine was analyzed for the presence of the drug. When the sample was mapped, no unassociated nanoparticle could be found in solution, indicating a successful interaction with the particles (Cytoviva, email communication). The spectra are shown in Figure 5. The mixture of hydralazine with the nanoparticles shows characteristics of both the pure drug and the particles. Because there is free hydralazine in the solution, the spectrum is closer to that of pure hydralazine than the nanoparticles.

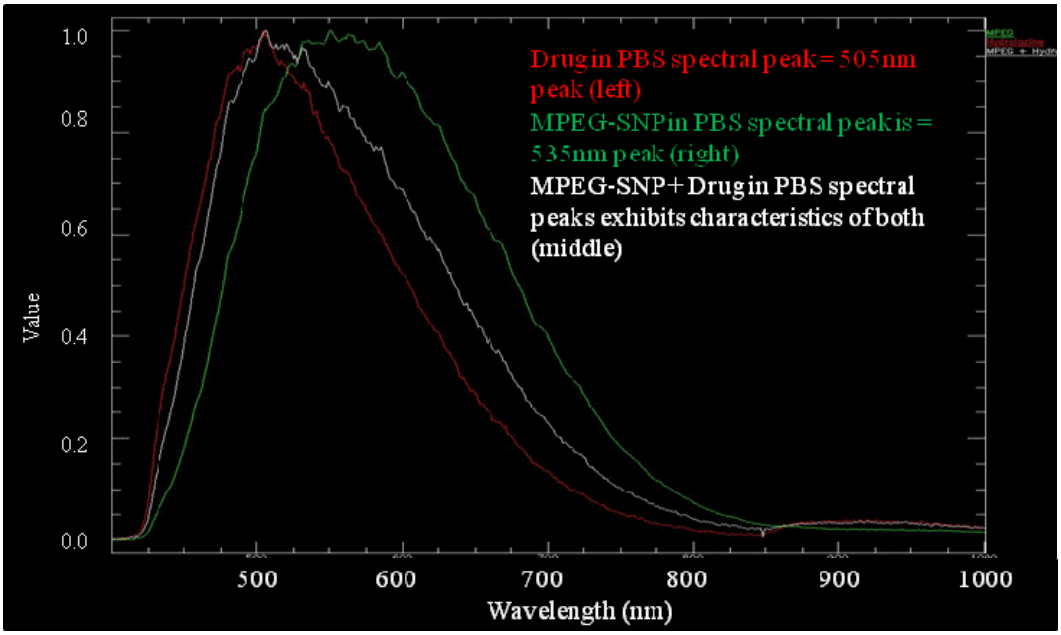

Figure 5. Spectra of hydralazine-loaded nanoparticles via reflective hyperspectral imaging. X-axis shows wavelength from 400-1000 nm. The right spectrum is the mPEG-Am modified nanoparticles; the left spectrum is that of hydralazine, and the middle spectrum is the mixture of the two. Image and analysis provided by Cytoviva, Inc. (Arab, AL).

3.3 Characterization of mPEG-Hz modified nanoparticles

The hydrazide particles have a particular advantage not present with the amine-modified particles. The active group of hydralazine is an azine, or R-NH-NH_2 off an aromatic phthalazine, and its hypertension activity stems from the phthalazine. The mPEG-hydrazide contains a similar group, but the aromatic part has been replaced by PEG and a carbonyl (C=O) in the R position of R-NH-NH_2. This may help the reactivity of the azine, as the carbonyl withdraws electrons from the azine, making it more nucleophilic. Because its reactivity is higher than that of amine groups, hydrazides are often used for bioconjugations. Therefore, the hydrazide group on the end of the mPEG may actively scavenge acrolein without the need for drug loading and possible side effects from using hydralazine.

Similar to the amine-modified particles, after synthesis, the hydrazide-modified particles were measured using dynamic light scattering (Figure 6). The particles have an average initial size of 20.26 nm in diameter with a PDI of 0.071. After storing them for over six months, they continue to be stable in solution.

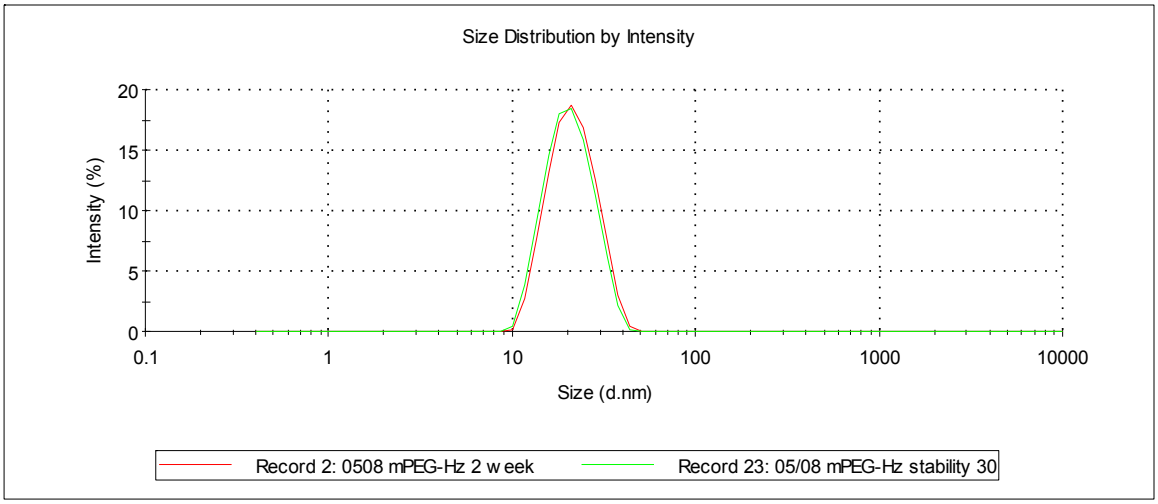

Figure 6. Size of Si-mPEG-Hz NP's both after synthesis and 30 weeks (6.5 months) of storage at room temperature. The particles have a narrow size distribution and retain their integrity over time.

Similar to the mPEG-Am particles, the particles remain stable for long periods of time in the basic pH, but their size and zeta potential were measured in water and PBS at pH 7 (Table 2). The hydrazide-modified particles have a higher zeta potential than their amine-modified counterparts, more than likely due to the increased amine groups on the end of the hydrazide PEG.

Table 2. Size and Zeta Potential of mPEG-Hz modified nanoparticles.

Temp. (ºC)	Solution	Diameter (nm)	PDI	Zeta Potential (mV) (St.Dev)	Zeta of Non-PEG sample (mV)
25	Water	23.00	0.128	-29.5 (4.8)	-31.7 (6.9)
25	PBS	28.33	0.281	-22.2 (2.0)	-25.4 (1.2)
37	Water	22.49	0.149	-22.3 (2.4)	-29.3 (0.7)
37	PBS	26.24	0.192	-21.4 (1.6)	-23.4 (0.8)

3.4 LDH permeability assay

An additional important factor in using a nanoparticle-based delivery system is the potential toxicity of the delivery system. Particularly for silica nanoparticles, some studies have showed cytotoxic effects. Studies with them have found that both very small and very large particles tend to create toxicity problems. On the other hand, particles in the sub-micron range exhibit a lower toxicity.[33–35] Because a neuron's membrane is essential to its function, the lactate dehydrogenase activity assay was chosen to measure toxicity. As the membrane integrity of the cells are compromised, the protein escapes from the cytoplasm. Therefore, higher activity indicates a higher level of membrane damage in the cell population. Triton X-100 was chosen as the positive control, and the cells within those wells had lysed after the incubation period. The LDH activity is measured relative to the vehicle control (PBS) as described in the methods, and none of the chosen nanoparticle concentrations showed significant cytotoxic effects (Figure 7).

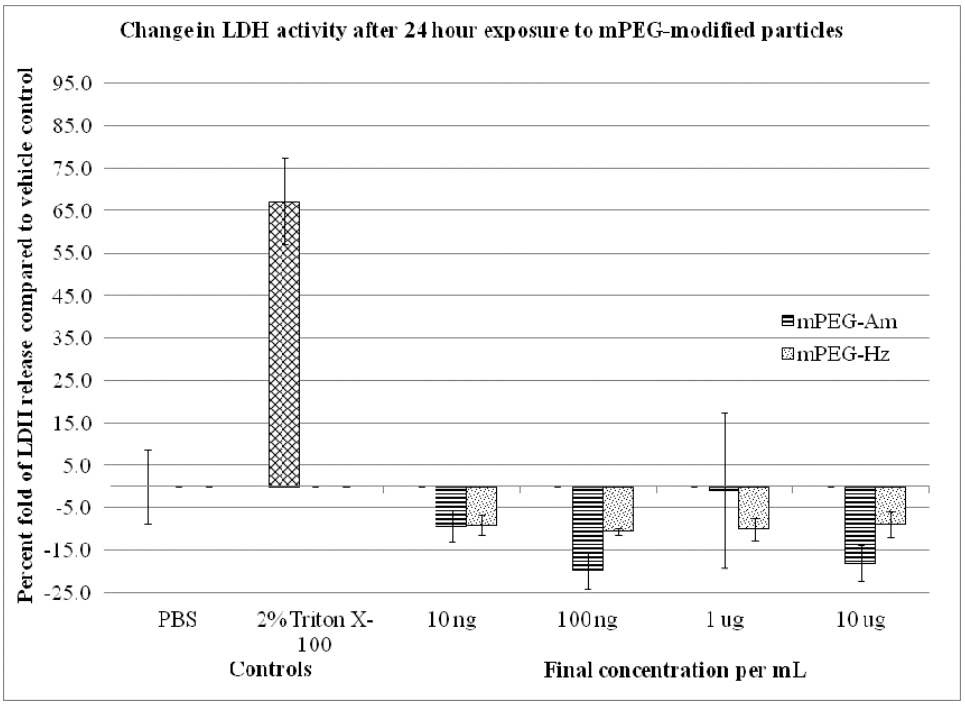

Figure 7. Lactate Dehydrogenase (LDH) assay in PC-12 cells. The two types of nanoparticles were incubated with PC-12 cells for 24 hours, and then the cell population was assayed. The nanoparticles did not show significant toxicity ($P < 0.01$) when compared to the vehicle control (PBS). The error bars show the standard deviation for each sample (n=3).

4. CONCLUSIONS

Much of the current state of the project focuses on the synthesis and characterization of the silica-based nanoparticles. This work demonstrates the feasibility of producing silica/polymer nanoparticles with a narrow size distribution using a facile synthesis scheme. The particles were characterized and showed prolonged stability in aqueous solutions. They also exhibited low toxicity *in vitro,* but the current toxicity methods are limited in that they measure the cells in bulk, and the data should be corroborated with single-cell analysis techniques such as flow cytometry or laser scanning cytometry, which analyzes each cell individually. Overall, the study is a step in the exploration of combining materials for use in nanomedical technology.

ACKNOWLEDGEMENTS

This research was funded by grants from the Christopher Columbus Foundation. Ms. White-Schenk is funded by an NSF graduate fellowship, grant DGE0833366.

REFERENCES

[1] Burke, D., Linden, R., Zhang, Y., Maiste, A., and Shields, C., "Incidence rates and populations at risk for spinal cord injury: A regional study," Spinal Cord 39(5), 274–278 (2001).

[2] Hamann, K., Nehrt, G., Ouyang, H., Duerstock, B., and Shi, R., "Hydralazine inhibits compression and acrolein-mediated injuries in ex vivo spinal cord," Journal of Neurochemistry 104(3), 708–718 (2008).

[3] Luo, J., Uchida, K., and Shi, R., "Accumulation of Acrolein–Protein Adducts after Traumatic Spinal Cord Injury," Neurochemical Research 30(3), 291–295 (2005).

[4] Liu-Snyder, P., McNally, H., Shi, R., and Borgens, R.B., "Acrolein-mediated mechanisms of neuronal death," Journal of Neuroscience Research 84(1), 209–218 (2006).

[5] Luo, J., and Shi, R., "Acrolein induces axolemmal disruption, oxidative stress, and mitochondrial impairment in spinal cord tissue," Neurochemistry International 44(7), 475–486 (2004).

[6] Shi, R., Luo, J., and Peasley, M., "Acrolein inflicts axonal membrane disruption and conduction loss in isolated guinea-pig spinal cord," Neuroscience 115(2), 337–340 (2002).

[7] Uchida, K., Kanematsu, M., Morimitsu, Y., Osawa, T., Noguchi, N., and Niki, E., "Acrolein Is a Product of Lipid Peroxidation Reaction," Journal of Biological Chemistry 273(26), 16058 –16066 (1998).
[8] Hamann, K., Durkes, A., Ouyang, H., Uchida, K., Pond, A., and Shi, R., "Critical role of acrolein in secondary injury following ex vivo spinal cord trauma," Journal of Neurochemistry 107, 712–721 (2008).
[9] Liu-Snyder, P., Logan, M.P., Shi, R., Smith, D.T., and Borgens, R.B., "Neuroprotection from secondary injury by polyethylene glycol requires its internalization," Journal of Experimental Biology 210, 1455–1462 (2007).
[10] Zitting, A., and Heinonen, T., "Decrease of reduced glutathione in isolated rat hepatocytes caused by acrolein, acrylonitrile, and the thermal degradation products of styrene copolymers," Toxicology 17(3), 333–341 (1980).
[11] Liu-Snyder, P., Borgens, R.B., and Shi, R., "Hydralazine rescues PC12 cells from acrolein-mediated death," Journal of Neuroscience Research 84(1), 219–227 (2006).
[12] Cho, Y., Shi, R., Borgens, R.B., and Ivanisevic, A., "Functionalized mesoporous silica nanoparticle-based drug delivery system to rescue acrolein-mediated cell death," Nanomedicine 3, 507–519 (2008).
[13] Hamann, K., and Shi, R., "Acrolein scavenging: a potential novel mechanism of attenuating oxidative stress following spinal cord injury," Journal of Neurochemistry 111, 1348–1356 (2009).
[14] Leung, G., Sun, W., Zheng, L., Brookes, S., Tully, M., and Shi, R., "Anti-acrolein treatment improves behavioral outcome and alleviates myelin damage in experimental autoimmune enchephalomyelitis mouse," Neuroscience 173, 150–155 (2011).
[15] Cho, Y., Shi, R., and Borgens, R.B., "Chitosan produces potent neuroprotection and physiological recovery following traumatic spinal cord injury," Journal of Experimental Biology 213(9), 1513 –1520 (2010).
[16] Avgoustakis, K., Beletsi, A., Panagi, Z., Klepetsanis, P., Karydas, A.., and Ithakissios, D.., "PLGA–mPEG nanoparticles of cisplatin: in vitro nanoparticle degradation, in vitro drug release and in vivo drug residence in blood properties," Journal of Controlled Release 79, 123–135 (2002).
[17] Niidome, T., Yamagata, M., Okamoto, Y., Akiyama, Y., Takahashi, H., Kawano, T., Katayama, Y., and Niidome, Y., "PEG-modified gold nanorods with a stealth character for in vivo applications," Journal of Controlled Release: Official Journal of the Controlled Release Society 114(3), 343–347 (2006).
[18] Sashiwa, H., Yajima, H., and Aiba, S., "Synthesis of a Chitosan−Dendrimer Hybrid and Its Biodegradation," Biomacromolecules 4(5), 1244–1249 (2003).
[19] Zhang, C., Wängler, B., Morgenstern, B., Zentgraf, H., Eisenhut, M., Untenecker, H., Krüger, R., Huss, R., Seliger, C., et al., "Silica- and Alkoxysilane-Coated Ultrasmall Superparamagnetic Iron Oxide Particles: A Promising Tool To Label Cells for Magnetic Resonance Imaging," Langmuir 23(3), 1427–1434 (2006).
[20] Prow, T.W., Rose, W.A., Wang, N., Reece, L.M., Lvov, Y., and Leary, J.F., "Biosensor-controlled gene therapy/drug delivery with nanoparticles for nanomedicine," Proceedings of SPIE 5692(1), 199–208 (2005).
[21] Stöber, W., Fink, A., and Bohn, E., "Controlled growth of monodisperse silica spheres in the micron size range," Journal of Colloid and Interface Science 26(1), 62–69 (1968).
[22] Xu, H., Yan, F., Monson, E.E., and Kopelman, R., "Room-temperature preparation and characterization of poly (ethylene glycol)-coated silica nanoparticles for biomedical applications," Journal of Biomedical Materials Research Part A 66A(4), 870–879 (2003).
[23] He, Q., Zhang, J., Shi, J., Zhu, Z., Zhang, L., Bu, W., Guo, L., and Chen, Y., "The effect of PEGylation of mesoporous silica nanoparticles on nonspecific binding of serum proteins and cellular responses," Biomaterials 31(6), 1085–1092 (2010).
[24] Zhang, Z., Berns, A.E., Willbold, S., and Buitenhuis, J., "Synthesis of poly(ethylene glycol) (PEG)-grafted colloidal silica particles with improved stability in aqueous solvents," Journal of Colloid and Interface Science 310(2), 446–455 (2007).
[25] Bagwe, R.P., Hilliard, L.R., and Tan, W., "Surface Modification of Silica Nanoparticles to Reduce Aggregation and Nonspecific Binding," Langmuir 22, 4357–4362 (2006).
[26] Feng, L., Wang, Y., Wang, N., and Ma, Y., "Preparation of poly(ethylene glycol)-grafted silica nanoparticles using a facile esterification condensation method," Polymer Bulletin 63(3), 313–327 (2009).
[27] Peracchia, M.., Fattal, E., Desmaële, D., Besnard, M., Noël, J.., Gomis, J.., Appel, M., D' Angelo, J., and Couvreur, P., "Stealth® PEGylated polycyanoacrylate nanoparticles for intravenous administration and splenic targeting," Journal of Controlled Release 60(1), 121–128 (1999).
[28] Berriozabal, G., and De Miguel, Y.R., "Synthesis and characterisation of silica nanoparticles bearing different functional groups obtained via a two-stage method," physica status solidi (c) 7, 2692–2696 (2010).

[29] Cai, Q., Luo, Z.-S., Pang, W.-Q., Fan, Y.-W., Chen, X.-H., and Cui, F.-Z., "Dilute Solution Routes to Various Controllable Morphologies of MCM-41 Silica with a Basic Medium," Chemistry of Materials 13(2), 258–263 (2001).
[30] Bagwe, R.P., Yang, C., Hilliard, L.R., and Tan, W., "Optimization of Dye-Doped Silica Nanoparticles Prepared Using a Reverse Microemulsion Method," Langmuir 20(19), 8336–8342 (2004).
[31] Ma, K., Sai, H., and Wiesner, U., "Ultrasmall Sub-10 nm Near-Infrared Fluorescent Mesoporous Silica Nanoparticles," Journal of the American Chemical Society 134(32), 13180–13183 (2012).
[32] He, Q., Zhang, Z., Gao, F., Li, Y., and Shi, J., "In vivo Biodistribution and Urinary Excretion of Mesoporous Silica Nanoparticles: Effects of Particle Size and PEGylation," Small 7(2), 271–280 (2011).
[33] Medina, C., Jacoby, Malinski, Radomski, and Corbalan, J.J., "Amorphous silica nanoparticles trigger nitric oxide/peroxynitrite imbalance in human endothelial cells: inflammatory and cytotoxic effects," International Journal of Nanomedicine 7, 631 (2011).
[34] Napierska, D., Thomassen, L.C.J., Rabolli, V., Lison, D., Gonzalez, L., Kirsch-Volders, M., Martens, J.A., and Hoet, P.H., "Size-Dependent Cytotoxicity of Monodisperse Silica Nanoparticles in Human Endothelial Cells," Small 5, 846–853 (2009).
[35] Park, J.-H., Gu, L., Von Maltzahn, G., Ruoslahti, E., Bhatia, S.N., and Sailor, M.J., "Biodegradable luminescent porous silicon nanoparticles for in vivo applications," Nature Materials 8, 331–336 (2009).